RESEARCH ARTICLE

Magnetic Resonance Images Implicate That Glymphatic Alterations Mediate Cognitive Dysfunction in Alzheimer Disease

Jung-Lung Hsu, MD, PhD,[1,2,3] Yi-Chia Wei, MD, PhD,[4,5,6] Cheng Hong Toh, MD, PhD,[7] Ing-Tsung Hsiao, PhD,[8,9] Kun-Ju Lin, MD, PhD,[8,9] Tzu-Chen Yen, MD, PhD,[10] Ming-Feng Liao, MD, PhD,[2] and Long-Sun Ro, MD, PhD[2]

Objective: The glymphatic system cleans amyloid and tau proteins from the brain in animal studies of Alzheimer disease (AD). However, there is no direct evidence showing this in humans.
Methods: Participants (n = 50, 62.6 ± 5.4 years old, 36 women) with AD and normal controls underwent amyloid positron emission tomography (PET), tau PET, structural T1-weighted magnetic resonance imaging, and neuropsychological evaluation. Whole-brain glymphatic activity was measured by diffusion tensor image analysis along the perivascular space (DTI-ALPS).
Results: ALPS-indexes showed negative correlations with deposition of amyloid and tau on PET images and positive correlations with cognitive scores even after adjusting for age, sex, years of education, and *APOE4* genotype covariates in multiple AD-related brain regions (all $p < 0.05$). Mediation analysis showed that ALPS-index acted as a significant mediator between regional standardized uptake value ratios of amyloid and tau images and cognitive dysfunction even after correcting for multiple covariates in AD-related brain regions. These regions are responsible for attention, memory, and executive function, which are vulnerable to sleep deprivation.
Interpretation: Glymphatic system activity may act as a significant mediator in AD-related cognitive dysfunction even after adjusting for multiple covariates and gray matter volumes. ALPS-index may provide useful disease progression or treatment biomarkers for patients with AD as an indicator of modulation of glymphatic activity.

ANN NEUROL 2023;93:164–174

The glymphatic system is a novel clearance mechanism in the brain that is responsible for cerebrospinal fluid flow into the brain parenchyma along the arterial perivascular space and subsequently into the brain interstitial space, which transports solutes from the neuropil into meningeal and cervical lymphatic drainage vessels.[1] In animal studies, researchers have clarified that the glymphatic system contributes to 55 to 65% of β-amyloid protein clearance from the mouse brain.[2] Recently, Harrison et al showed that glymphatic clearance is related to cortical tau deposition in a mouse model of tauopathy.[3] According to the current hypothesis, amyloid and tau deposition could be the main pathologic process

View this article online at wileyonlinelibrary.com. DOI: 10.1002/ana.26516

Received Jun 23, 2022, and in revised form Oct 2, 2022. Accepted for publication Oct 2, 2022.

Address correspondence to Dr Ro, Department of Neurology, Chang Gung Memorial Hospital Linkou Medical Center and College of Medicine, Chang-Gung University, Linkou, Taoyuan, Taiwan. E-mail: cgrols@adm.cgmh.org.tw

From the [1]Department of Neurology, New Taipei Municipal TuCheng Hospital, New Taipei City, Taiwan; [2]Department of Neurology, Chang Gung Memorial Hospital Linkou Medical Center Neuroscience Research Center, and College of Medicine, Chang-Gung University, Taoyuan, Taiwan; [3]Taipei Medical University, Graduate Institute of Humanities in Medicine and Research Center for Brain and Consciousness, Shuang Ho Hospital, Taipei, Taiwan; [4]Department of Neurology, Chang Gung Memorial Hospital, Keelung, Taiwan; [5]Community Medicine Research Center, Chang Gung Memorial Hospital, Keelung, Taiwan; [6]Institute of Neuroscience, National Yang Ming Chiao Tung University, Taipei, Taiwan; [7]Department of Medical Imaging and Intervention, Chang Gung Memorial Hospital at Linkou, Chang Gung University College of Medicine, Taoyuan, Taiwan; [8]Department of Nuclear Medicine and Center for Advanced Molecular Imaging and Translation, Linkou Chang Gung Memorial Hospital, Taoyuan, Taiwan; [9]Department of Medical Imaging and Radiological Sciences and Healthy Aging Research Center, Chang Gung University, Taoyuan, Taiwan; and [10]APRINOIA Therapeutics, Taipei, Taiwan

contributing to cognitive dysfunction in patients with Alzheimer disease (AD).[4,5] Dysfunction in the glymphatic system has been proposed as the final common pathway for AD and other primary neurodegenerative diseases.[6]

Several magnetic resonance imaging (MRI) methods have been proposed to investigate the glymphatic system in humans.[7] A previous study used the intrathecal administration of gadolinium-based contrast agent (GBCA) as a tracer to study the glymphatic system in patients with normal pressure hydrocephalus (NPH).[8] An alternative method uses intravenous (IV) administration of GBCA to visualize enhancement in the perivascular space, especially in regions surrounding large cortical veins.[9] Recently, diffusion tensor image analysis along the perivascular space (DTI-ALPS) techniques have utilized diffusion MRI to estimate the activity of the glymphatic system by the ALPS-index.[10] DTI-ALPS provides a real-time method to evaluate the glymphatic system without the necessity of contrast agent use. Currently, it is the most widely used MRI technique to evaluate human glymphatic function and is significantly associated with the intrathecal method of glymphatic measurement.[11] ALPS-indexes have shown significant positive correlations with cognition scores in patients with AD and normal aging.[10,12] ALPS-index has also been studied in other diseases, such as NPH, type 2 diabetes mellitus, ischemic stroke, multiple sclerosis, and Parkinson disease.[13–17]

However, the associations between glymphatic activity and AD biomarkers have not been well studied in humans. Therefore, we hypothesize that glymphatic activity mediates the deposition of amyloid and tau proteins and thus affects cognitive dysfunction in patients with AD. This study combines amyloid and tau position emission tomography (PET) and MRI DTI-ALPS to explore associations between glymphatic activity and amyloid and tau deposition and cognitive dysfunction in patients with AD.

Materials and Methods

This is a cross-sectional study conducted at Linkou Chang Gung Memorial Hospital. The study protocol was approved by the institutional review board (CGMHIRB No. 201801828B0A3, 201802151A0). Written informed consent was obtained from each participant before the study procedure. Each participant completed cognitive evaluation, brain MRI, ^{18}F-AV-45 (florbetapir) PET, and ^{18}F-APN1607 (also known as florzolotau) PET scans. In addition, ^{18}F-AV-45 PET imaging results were used as the inclusion criteria to confirm the presence and absence of amyloid deposition in AD patients and normal controls (NCs).

Subjects

A total of 50 participants, including 13 NCs and 37 patients with AD, were recruited for this study. The diagnosis of mild to moderate AD was based on the National Institute on Aging/Alzheimer's Association research framework.[5] Neuropsychological assessments were performed in all participants, including the Mini-Mental State Examination (MMSE), the Clinical Dementia Rating (CDR) scale, and the Consortium to Establish a Registry for Alzheimer's Disease Neuropsychological Assessment Battery (CERAD-NAB) total scores (range = 0–100), with greater scores indicating better cognition.[18–22] The CDR sum of boxes scores graded for disease severity. The presence of the ε2, ε3, and ε4 alleles of the apolipoprotein E (*APOE*) gene was determined by assessing the sequences at 2 single-nucleotide polymorphisms (rs429358 and rs7412).[23] NCs in the study were required to be 20 to 80 years old with normal cognitive function (CDR: 0; MMSE: 26–30; negative ^{18}F-AV-45 PET result).

Image Acquisition

^{18}F-AV-45 radiosynthesis and PET data acquisition were performed according to our previous protocols.[24] All participants underwent ^{18}F-AV-45 PET scans on an integrated PET/MRI system (Siemens Biograph mMR scanner). Scanning times for all participants were between 11:00 and 15:00. PET images were acquired after IV injection of 374 ± 21MBq of ^{18}F-AV-45. A 10-minute scan was acquired starting at 50 minutes after the tracer injection. The PET images were obtained using attenuation correction procedures and imaging reconstruction methods based on the software version VB20 provided by the manufacturer. The reconstructed images had a matrix size of 334 × 334 × 127 and a voxel size of 0.83 × 0.83 × 1.2mm^3.

^{18}F-APN1607 was prepared and synthesized at the cyclotron facility of Chang Gung Memorial Hospital.[25] All participants were studied in a Biograph mCT PET/computed tomography system (Siemens Medical Solutions, Malvern, PA) with an interval of at least 2 weeks from the ^{18}F-AV-45 PET scan. Scanning times for all participants were between 15:00 and 16:00. For the ^{18}F-APN1607 PET study, a 10-minute scan was acquired 90 minutes after an injection of 185 ± 74MBq of ^{18}F-APN1607. PET images were reconstructed using the same method as above. The reconstructed images had a matrix size of 400 × 400 × 148 and a voxel size of 0.68 × 0.68 × 1.5mm^3.

The MRI protocol in PET/MRI included a sagittal fluid attenuation inversion recovery sequence (repetition time [TR] = 6,000 milliseconds, echo time [TE] = 392 milliseconds, inversion time [TI] = 2,100 milliseconds, voxel size = 0.5 × 0.5 × 1mm^3) and a whole-brain axial 3-dimensional T1-weighted magnetization-prepared rapid acquisition gradient echo sequence (TR = 2,000 milliseconds, TE = 2.67 milliseconds, TI = 900 milliseconds, flip angle = 9°, voxel size = 1 × 1 × 1mm^3). For the whole-head diffusion study, the diffusion tensor image sequence was acquired along 64 gradient directions for b = 1,000s/mm^2 with an echo planar imaging sequence with TR = 8,800 milliseconds, TE = 91 milliseconds, matrix = 116 × 116, field of view = 256 × 256 mm^2, 70 slices, slice thickness = 2.2mm, no gap, and number of excitations = 1. One b = 0s/mm^2 image was acquired with the diffusion-weighted imaging (DWI) sequence.

Image Analysis

For each participant, we registered both ^{18}F-AV-45 and ^{18}F-APN1607 images to individual T1-weighted MRI images using the SPM12 toolbox.[26] This procedure ensured each PET image was in alignment with the native MRI scans. The Muller–Gartner method was used for partial volume correction.[27] Then, the high-resolution T1-weighted MRI scans in native space were normalized to the Montreal Neurological Institute (MNI) standard space using the Computational Anatomy Toolbox.[28] This transform matrix was applied to PET images. The averaged intensity across the whole cerebellum was used as the reference for the ^{18}F-AV-45 PET images. For ^{18}F-APN1607 images, we used the technique known as parametric estimation of reference signal intensity to perform count normalization by using the white matter as the reference region.[29] Eighteen regions of interest (ROIs), including the bilateral frontal, parietal, temporal, occipital lobes, anterior and posterior cingulate cortex , precuneus, parahippocampus and sensory–motor cortex, were selected based on the Harvard–Oxford cortical structural atlas, and the average values from both sides were used for subsequent analysis.[30] Finally, the regional standardized uptake value ratios (SUVRs) from both PET images were calculated by using the mean intensity in the target ROIs divided by the averaged intensity of the reference regions.

To study the gray matter (GM) ratio in the patients with AD and NCs, we calculated the total modulated GM volumes (GMVs) and the regional GMVs in the target ROIs, which were then divided by the individual total intracranial volume (ICV) for the total and regional GMV ratios. Higher GMV ratios represented large brain volumes. Diffusion MRI data analysis was performed by using ExploreDTI.[31] The DWI datasets were coregistered to native T1-weighted images. Then, the resulting DWI data were fitted to the DTI model.[32] A fractional anisotropy (FA) map of each participant was coregistered to the FA map template of the International Consortium of Brain Mapping (ICBM) DTI-81 Atlas in MNI space, and the accuracy of coregistration was visually confirmed. The ICBM DTI-81 Atlas had the labels of the projection (superior and posterior corona

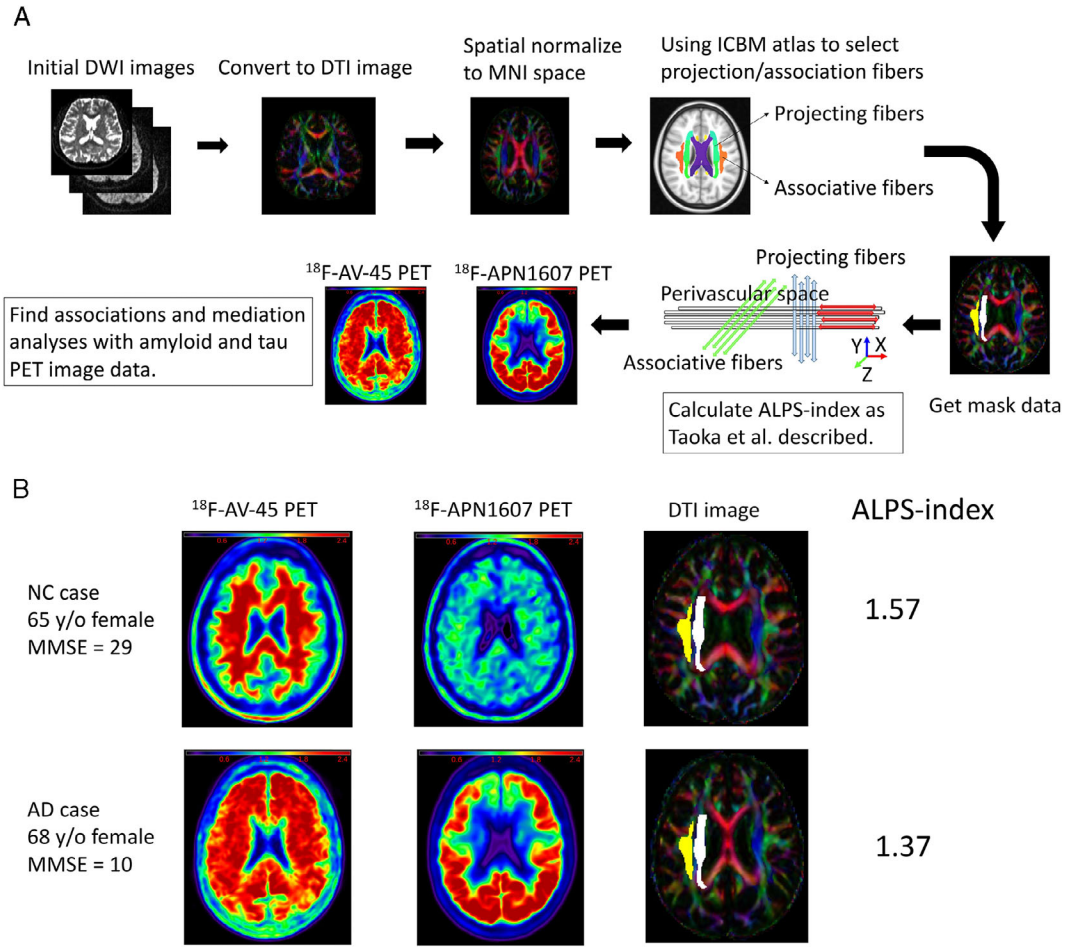

FIGURE 1: Schema shows the analysis process and data from two representative participants. (A) Analysis process from initial diffusion-weighted imaging (DWI) images to calculate analysis along the perivascular space (ALPS) indexes and evaluate the associations with standardized uptake value ratios of amyloid (^{18}F-AV-45) position emission tomography (PET) images and tau (^{18}F-APN 1607) PET images. (B) Images and data from 2 representative participants show the ^{18}F-AV-45 PET images, ^{18}F-APN 1607 PET images, diffusion tensor imaging (DTI) images, and ALPS-indexes. AD = Alzheimer disease; ICBM = International Consortium of Brain Mapping; MMSE = Mini-Mental State Examination; MNI = Montreal Neurological Institute; NC = normal control; y/o = years old.

radiata) and association (superior longitudinal fasciculus) fibers in the periventricular area. We extracted the periventricular projection and association fibers within the 25- to 33mm range above the anterior–posterior commissure line in MNI space, where the x-axis line corresponded to the passing direction of the vessels in the deep white matter. ALPS-index and diffusivity from projection and association fibers derived from the ICBM DTI-81 Atlas were calculated as Taoka et al described.[10] Higher ALPS-index represented better glymphatic activity. Figure 1 shows the schema of the DTI analysis process and images and data from 2 representative participants.

Statistical Analyses

All statistical analyses were performed using SPSS (v21.0; IBM, Armonk, NY). Continuous variables are expressed as the mean ± standard deviation. Nonparametric Mann–Whitney *U* tests and χ^2/Fisher exact tests were performed between AD patients and NCs whenever appropriate. Regression analyses of the associations between ALPS-indexes and mean regional SUVR values in the ^{18}F-AV-45 PET images and ^{18}F-APN1607 PET images and cognition were performed. Age, sex, years of education, and *APOE4* genotype were used as covariates. To study the sequential changes in regional SUVRs in each PET image, ALPS-indexes, and regional GMV ratio, we scaled the above data to 0–100%, with 0% representing minimal abnormalities and 100% representing maximal abnormalities. We applied a nonlinear curve fitting model to investigate the relationships between SUVRs of amyloid and tau, ALPS-indexes, GMV ratios, and CERAD-NAB total scores using Prism software (v5.0; GraphPad San Diego, CA). Mediation analysis is a statistical model used to quantify a mediating variable in the causal sequence by which an antecedent variable causes a dependent variable[33] and was performed using the PROCESS macro for SPSS (model 4) with a level of confidence at 95% and 5,000 bootstrap samples.[34] To explore the significance of ALPS-index as a mediator between regional SUVRs in both PET images and CERAD-NAB total scores and GMV ratios, we used age, sex, education years, and *APOE4* genotype as covariates. Mediation analysis comprised total, direct, and indirect effects. The percent of mediation (Pm) calculated by indirect effect divided by total effect was performed to study the weight of ALPS-index in the total effect. Statistical significance was defined as a p value < 0.05.

Results

Demographic Data

Table 1 shows the demographic data of 37 patients with AD and 13 NCs. The mean age of patients with AD showed no significant difference from NCs (mean age of patients with AD = 63.2 ± 4.7 years, mean age of NCs = 61.0 ± 7.1 years, $p = 0.22$). No significant group differences in sex, education years, *APOE4* genotype, or total ICV differences were found ($p = 0.79$, $p = 0.70$, $p = 0.18$, and $p = 0.85$, respectively). However,

TABLE 1. Demographic Data of Patients with AD and NCs

Characteristic	NCs (n = 13)	AD (n = 37)	*p*
Mean age, yr	61.0 ± 7.1	63.2 ± 4.7	0.31
Sex, male:female	4:9	10:27	0.79
Education, yr	10.5 ± 3.5	10.9 ± 3.5	0.70
Onset to scan time, yr	—	3.9 ± 1.8	
Mean MMSE score	28.0 ± 1.2	17.7 ± 6.7	<0.01
Mean CERAD-NAB total score	81.2 ± 9.6	47.4 ± 18.3	<0.01
Mean CDR-SB score	0.0 ± 0.0	0.9 ± 0.4	<0.01
APOE4 genotype (positive:negative)	2:11	13:24	0.18
Mean cortical SUVRs of ^{18}F-AV-45	1.1 ± 0.1	1.7 ± 0.3	<0.01
Mean cortical SUVRs of ^{18}F-APN1607	0.9 ± 0.1	1.8 ± 0.4	<0.01
Mean total GMV ratio, %	41.4 ± 2.8	36.2 ± 3.3	<0.01
Mean total ICV, ml	1,345.6 ± 143.4	1,353.7 ± 128.9	0.83
Mean ALPS indexes	1.5 ± 0.1	1.4 ± 0.2	0.04

AD = Alzheimer disease; ALPS = diffusion tensor image analysis along the perivascular space; *APOE* = apolipoprotein E; CDR-SB = Clinical Dementia Rating sum of boxes; CERAD-NAB = Consortium to Establish a Registry for Alzheimer's Disease Neuropsychological Assessment Battery; GMV = gray matter volume; ICV = intracranial volume; MMSE = Mini-Mental State Examination; NC = normal control; SUVR = standardized uptake value ratio.

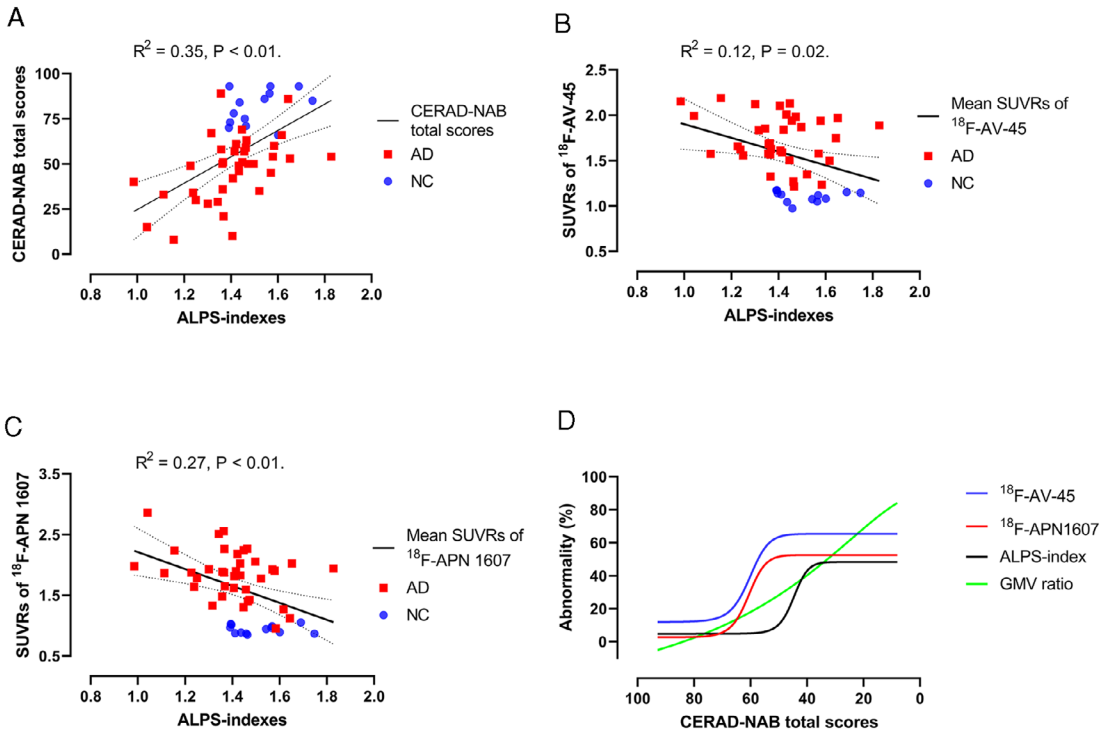

FIGURE 2: Diffusion tensor image analysis along the perivascular space (ALPS) indexes are correlated with the mean standardized uptake value ratios (SUVRs) of ^{18}F-AV-45 PET images and ^{18}F-APN 1607 position emission tomography (PET) images and Consortium to Establish a Registry for Alzheimer's Disease Neuropsychological Assessment Battery (CERAD-NAB) total scores. (A) ALPS-indexes showed a significant correlation with CERAD-NAB total scores after adjusting for age, sex, years of education, and *APOE4* genotype ($R^2 = 0.35$, $p < 0.01$). (B) ALPS-indexes showed a significant correlation with the mean SUVRs of ^{18}F-AV-45 PET images after adjusting for age, sex, years of education, and *APOE4* genotype ($R^2 = 0.12$, $p = 0.02$). (C) ALPS-indexes showed a significant correlation with the mean SUVRs of ^{18}F-APN 1607 PET images after adjusting for age, sex, years of education, and *APOE4* genotype ($R^2 = 0.27$, $p < 0.01$). Dotted lines indicate the 95% confidence intervals. (D) Combined fitting curves from the SUVRs of the ^{18}F-AV-45 PET image, SUVRs of the ^{18}F-APN1607 PET image, ALPS-indexes, and gray matter volume (GMV) ratios in the precuneus region. The values of regional SUVRs in the ^{18}F-AV-45 PET images and ^{18}F-APN1607 PET images were scaled to 0–100%, with 0% representing the minimal value and 100% representing the maximal value. The original ALPS-indexes and regional GM ratios were reversed, with 100% representing the minimal value and 0% representing the maximal value. This normalization procedure made the higher values of abnormalities in regional SUVRs, GMV ratios, and ALPS-indexes represent the more severe disease state. AD = Alzheimer disease; NC = normal control.

significantly lower MMSE scores, CERAD-NAB total scores, and total GMV ratios were found in patients with AD than in NCs (all $p < 0.01$). The mean cortical SUVRs of ^{18}F-AV-45, ^{18}F-APN1607, and ALPS-indexes showed significant differences between patients with AD and NCs ($p < 0.01$, $p < 0.01$, and $p = 0.04$, respectively).

ALPS-index associated with amyloid and tau deposition GMV ratios and cognition

The total GMV ratios showed a significantly positive correlation with CERAD-NAB total scores ($R^2 = 0.61$, $p < 0.01$). The ALPS-indexes showed significantly positive correlations with CERAD-NAB total scores ($R^2 = 0.35$, $p < 0.01$), MMSE scores ($R^2 = 0.33$, $p < 0.01$), and total GMV ratios ($R^2 = 0.27$, $p < 0.01$; Fig 2A). The ALPS-indexes showed significantly negative correlations with mean values of regional SUVRs in the ^{18}F-AV-45 PET images ($R^2 = 0.12$, $p = 0.02$) and ^{18}F-APN1607 PET images ($R^2 = 0.27$, $p < 0.01$; see Fig 2B,C). Notably, the ALPS index–SUVR correlations in both sets of PET images existed in multiple ROIs but not in the parahippocampus ($p = 0.31$ and $p = 0.07$, respectively). In addition, the ALPS index–GMV ratio correlations existed in most ROIs except in the anterior cingulate cortex and sensory–motor cortex ($p = 0.22$ and $p = 0.06$, respectively; Table 2).

Sequential changes in SUVRs in ^{18}F-AV-45 and ^{18}F-APN1607 PET images, regional GMV ratios, and ALPS-indexes in relation to cognitive dysfunction

The precuneus region is one of the earliest affected regions in AD and was selected to study the sequential changes in amyloid and tau deposition, GMV ratios, and glymphatic activity according to the severity of cognitive dysfunction. A sigmoidal 4-parameter logistic curve fitting model

TABLE 2. Regression Analysis between ALPS Indexes and Regional SUVRs of ^{18}F-AV-45 and ^{18}F-APN1607 PET Imaging and GMV Ratios after Correction for Age, Sex, Education Years and *APOE4* Genotype

	Mean SUVRs of ^{18}F-AV-45		Mean SUVRs of ^{18}F-APN1607		GMV Ratios	
Regions	R^2	p	R^2	p	R^2	p
F	0.12	0.03	0.23	<0.01	0.14	0.03
P	0.12	0.03	0.29	<0.01	0.26	< 0.01
T	0.11	0.03	0.25	<0.01	0.31	<0.01
O	0.20	<0.01	0.34	<0.01	0.21	<0.01
pHP	0.06	0.31	0.16	0.07	0.15	0.02
ACC	0.10	0.04	0.30	<0.01	0.25	0.22
PCC	0.14	0.01	0.30	<0.01	0.16	<0.01
PreCu	0.16	<0.01	0.33	<0.01	0.10	0.03
S-M	0.16	<0.01	0.31	<0.01	0.17	0.06

ACC, anterior cingulate cortex; ALPS, diffusion tensor image analysis along the perivascular space; *APOE*, apolipoprotein E; F, frontal; GMV, gray matter volume; O, occipital; P, parietal; PCC, posterior cingulate cortex; PET = positron emission tomography; pHP, parahippocampus; PreCu, precuneus; S-M, sensory–motor cortex; SUVR, standardized uptake value ratio; T, temporal.

showed that both fitting curves for SUVRs from the ^{18}F-AV-45 and ^{18}F-APN1607 PET images gradually increased and then reached a plateau (see Fig 2D). The trajectory of ALPS-indexes resembled the curves of both PET images but appeared later. The fitted curve of regional GMV ratios showed a relatively linear increasing curve versus the decrease in CERAD-NAB total scores. By quantitative analysis, the CERAD-NAB total scores at the inflection points of the sigmoidal curves were higher in ^{18}F-AV-45 PET images (61.2) followed by ^{18}F-APN1607 PET images (60.9), ALPS-indexes (45.5), and GMV ratios (38.6), indicating that the accelerating turning points in ALPS-indexes might occur later than changes in amyloid and tau deposition but earlier than the changes in GMV ratios. This was the rationale to put the ALPS-index in the mediator role in a statistical model of mediation analysis.

ALPS-index as a significant mediator between deposition of amyloid and tau proteins, cognitive dysfunction, and GMV ratios

In the mediation analysis for amyloid deposition in the precuneus region, the ALPS-index showed significant mediation effects between the regional SUVRs of ^{18}F-AV-45 PET images and CERAD-NAB total scores after correcting for multiple covariates (Pm = 16.86%; total effect B = −27.66, $p < 0.001$; direct effect B = −23.00, $p < 0.001$; indirect effect B = −4.66, 95% confidence interval [CI] = −9.81 to −0.95). In the tau study, the ALPS-index also showed significant mediation effects between the regional SUVRs of ^{18}F-APN1607 PET images and CERAD-NAB total scores (Pm = 11.37%; total effect B = −19.56, $p < 0.001$; direct effect B = −17.34, $p < 0.001$; indirect effect B = −2.23, 95% CI = −5.30 to −0.12; Fig 3A).

For AD-related brain regions, Figure 3B,D shows the Pm of ALPS-indexes in the relationship between regional amyloid and tau deposition and cognitive dysfunction. In the amyloid study, the glymphatic activity measured by ALPS-index was a significant mediator weighing Pm at approximately 16.34 to 18.93% of the total effect in most brain regions, except the parahippocampal region. In the tau study, the ALPS-indexes significantly mediated in most brain regions, except the occipital region, with a weighting Pm of approximately 11.37 to 24.98% of the total effect.

In the mediation analysis of ALPS-indexes between regional amyloid/tau deposition and GMV ratios, the total effects were significant in all brain regions. However, the ALPS-indexes showed mediation effects only in the parietal and temporal regions (Pm ranged from 13.71 to 17.86%; see Fig 3E).

ALPS-index as a significant mediator in cognitive dysfunction after correction for GMV ratios

Because the regional GMV ratios showed significant correlations with ALPS-indexes and CERAD-NAB total scores (see Table 2), we further controlled for the regional GMV

ratios in addition to the original covariates to study the mediation effects of ALPS-indexes between SUVRs of ^{18}F-AV-45 and ^{18}F-APN1607 PET images and CERAD-NAB total scores (Fig 4). The total effects in the amyloid and tau studies were significant in most of the ROIs (B ranged from −14.47 to −39.52 in the amyloid study

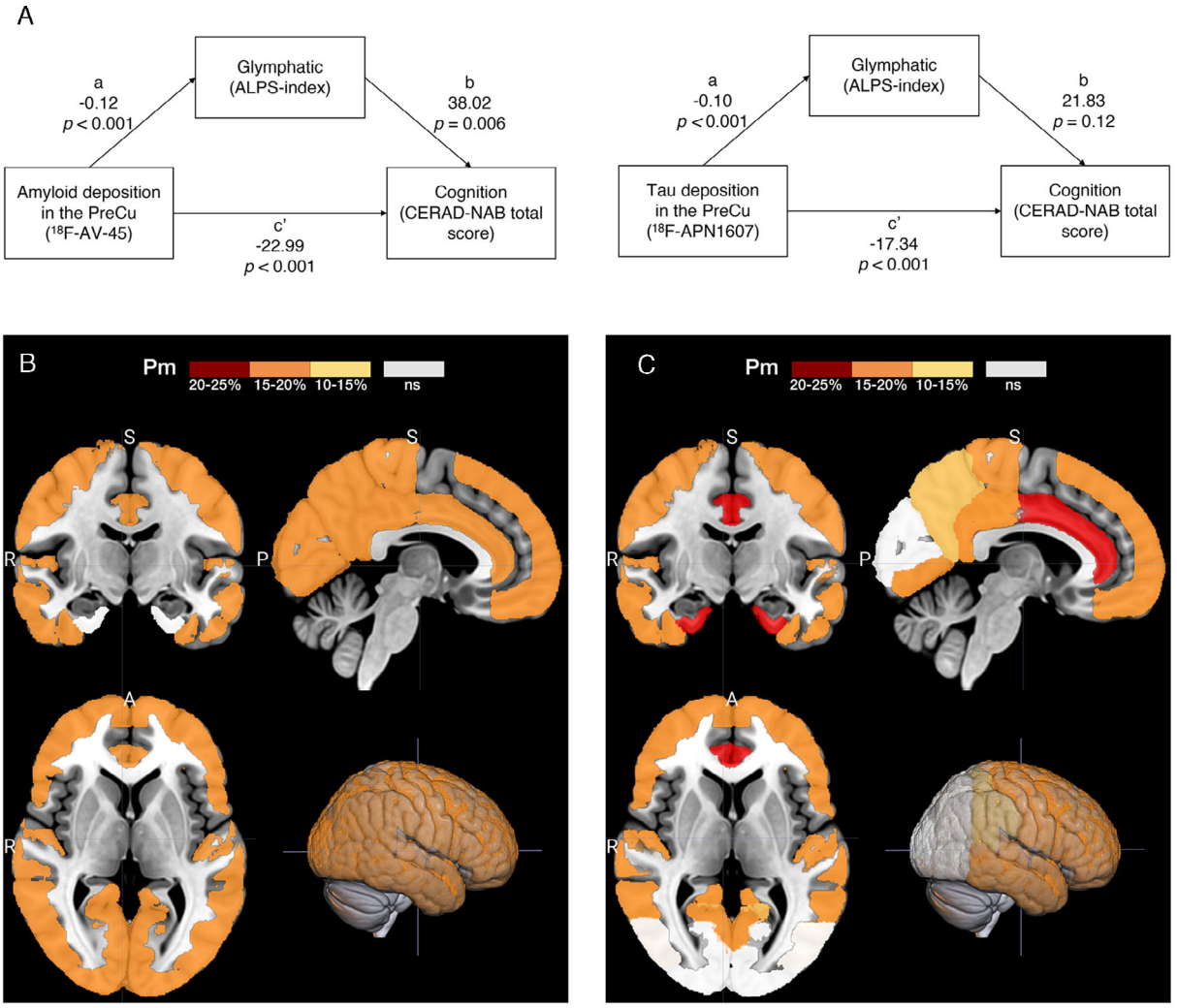

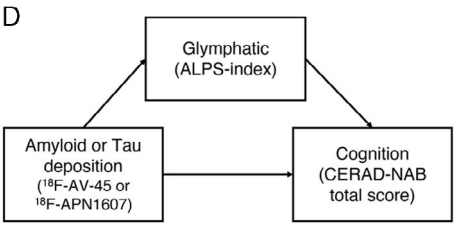

Pm(%) of ALPS-index between regional amyloid/tau and cognition

	F	P	T	O	pHP	ACC	PCC	PreCu	S-M
Amyloid	17.09	18.38	16.90	17.87		18.93	17.87	16.86	16.34
Tau	18.56	13.88	17.13		21.00	24.98	17.54	11.37	15.79

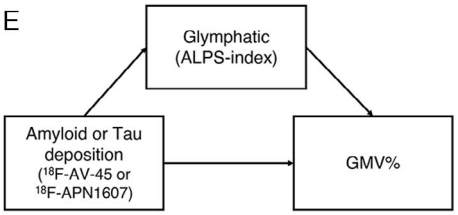

Pm(%) of ALPS-index between regional amyloid/tau and GMV%

	F	P	T	O	pHP	ACC	PCC	PreCu	S-M
Amyloid		17.86	17.17						
Tau		13.71	14.41						

(Figure legend continues on next page.)

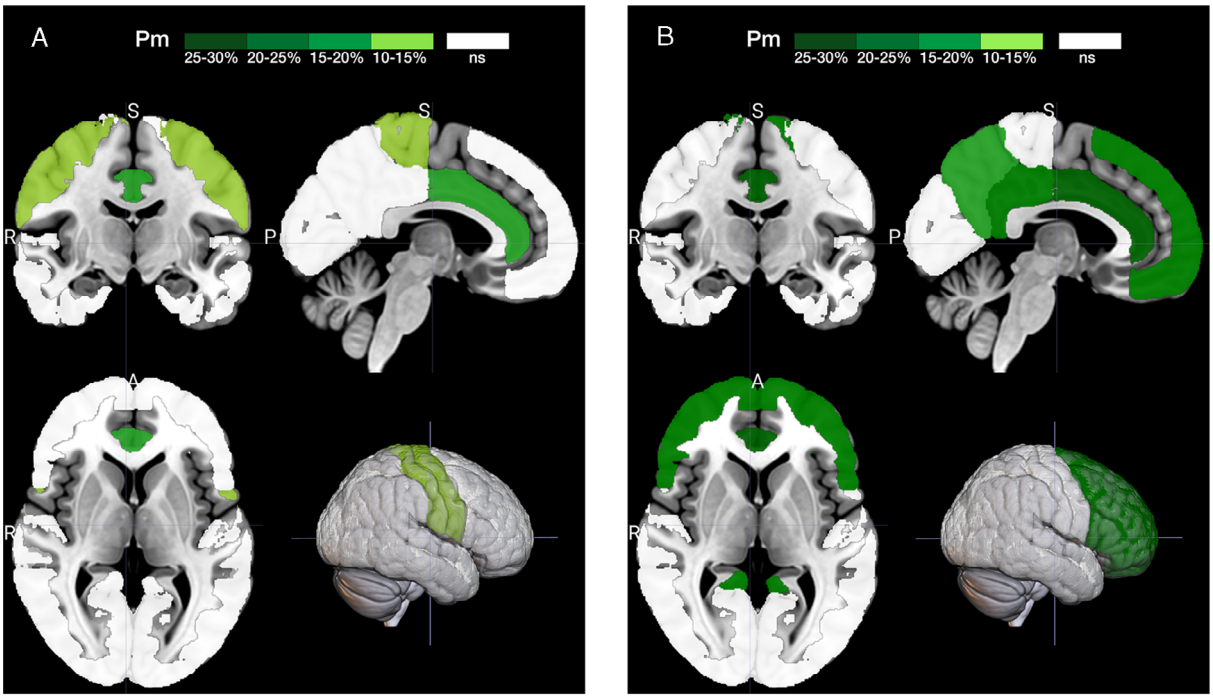

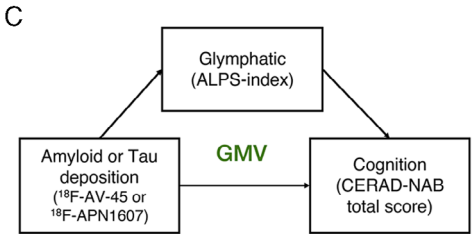

Pm(%) of ALPS-index between regional amyloid/tau and cognition (Adjusted for regional GMV%)

	F	P	T	O	pHP	ACC	PCC	PreCu	S-M
A						17.51			14.40
T	21.78					25.08	24.46	15.14	

FIGURE 4: Topographical distribution of diffusion tensor image analysis along the perivascular space (ALPS) indexes as significant mediators after correction for age, sex, years of education, *APOE4* genotype, and regional gray matter volume (GMV) ratios. (A, B) The ALPS-index significantly mediates the relationship between amyloid (A) and tau (B) deposition and cognitive dysfunction after correction for multiple covariates. A = anterior; P = posterior; R = right; S = superior. (C) The percent of mediation (Pm) of ALPS-indexes between regional amyloid (A) and tau (T) deposition and cognition from the indirect mediation analysis. The significant regions are plotted on the different color bars. Nonsignificant (ns) regions are in white. Background regions are in gray. ACC = anterior cingulate cortex; CERAD-NAB = Consortium to Establish a Registry for Alzheimer's Disease Neuropsychological Assessment Battery; F = frontal; O = occipital; P = parietal; PCC = posterior cingulate cortex; pHP = parahippocampus; PreCu = precuneus; S-M = sensory–motor cortex; T = temporal.

and from −9.47 to −36.65 in the tau study, all $p < 0.05$) except the parahippocampal region ($p = 0.63$ and 0.37, respectively). From indirect analysis of the amyloid study, ALPS-indexes showed significant mediation effects in the anterior cingulate cortex (indirect effect B = −5.04, 95% CI = −10.97 to −0.72) and the sensory–motor cortex (B = −5.69, 95% CI = −11.78 to −0.77; see Fig 4A,C). In the tau study, ALPS-indexes showed significant

FIGURE 3: The schema of mediation analysis in the precuneus region and the topographical distribution of diffusion tensor image analysis along the perivascular space (ALPS) indexes as significant mediators after correction for age, sex, years of education and *APOE4* genotype. (A). ALPS-indexes are statistically significant mediators of the relationship between amyloid position emission tomography (PET), tau PET, and cognitive dysfunction in the precuneus. (B, C) The ALPS-index significantly mediates the relationship between amyloid (A) and tau (B) deposition and cognitive dysfunction. A = anterior; P = posterior; R = right; S = superior. (D) The percent of mediation (Pm) analysis of ALPS-indexes between regional amyloid and tau deposition and cognition from the indirect mediation analysis. (E) The Pm of ALPS-indexes between regional amyloid and tau and gray matter volume (GMV) ratios. The significant regions are plotted on the different color bars. Nonsignificant (ns) regions are in white. Background regions are in gray. ACC = anterior cingulate cortex; CERAD-NAB = Consortium to Establish a Registry for Alzheimer's Disease Neuropsychological Assessment Battery; F = frontal; O = occipital; P = parietal; PCC = posterior cingulate cortex; pHP = parahippocampus; PreCu = precuneus; S-M = sensory–motor cortex; T = temporal.

mediation effects in the frontal region (indirect effect B = −4.29, 95% CI = −9.87 to −0.73), anterior cingulate cortex (B = −8.73, 95% CI = −18.15 to −1.86), posterior cingulate cortex (B = −2.32, 95% CI = −5.84 to −0.27), and precuneus (B = −2.32, 95% CI = −5.64 to −0.05; see Fig 4B,C).

Discussion

This is a pioneering human study that explores the role of glymphatic activity in the relationship between the deposition of amyloid and tau proteins and cognitive dysfunction. We used the regional SUVRs of ^{18}F-AV-45 PET images and ^{18}F-APN1607 PET images to represent the burden of amyloid and tau deposition in patients with AD. In contrast, the ALPS-indexes represent a surrogate biomarker of glymphatic system activity.[10] Our findings suggest that ALPS-indexes showed significantly negative correlations with amyloid and tau burden but demonstrated positive correlations with CERAD-NAB total scores and GMV ratios. In addition, after indirect analysis, ALPS-index served as a significant mediator in the relationships between the regional SUVRs of ^{18}F-AV-45 PET images and ^{18}F-APN1607 PET images and CERAD-NAB total scores in many brain regions even after correction for multiple covariates. The current study indicates that ALPS-index acts as a significant mediator in the relationship between the burden of amyloid and tau proteins and cognitive dysfunction.

Glymphatic activity correlates with biomarkers of AD and is a significant mediator in AD-related cognitive dysfunction

Previous studies have shown that ALPS-indexes had significant correlations with cognitive scores in patients with AD, individuals with mild cognitive impairment, and elderly individuals with normal cognition,[10,35,36] which is consistent with our finding that ALPS-indexes showed significantly positive correlations with CERAD-NAB total scores in patients with AD. Furthermore, ALPS-indexes showed significantly negative correlations with amyloid and tau protein deposition. It is known that the glymphatic system contributes to the clearance of waste products in the brain.[37,38] In animal studies, the glymphatic system is responsible for the clearance of β-amyloid protein and tau proteins.[2,3] However, there are few direct human studies reported in the English literature. Our findings might provide evidence that glymphatic activity is correlated with amyloid and tau protein deposition in the brain. We further investigated the mediating role of glymphatic activity in the relationship between the burden of amyloid and tau proteins and cognitive dysfunction. Previous studies have shown that amyloid and tau PET images are associated with cognitive scores in patients with AD.[39–41] In studying sequential changes in amyloid, tau, and ALPS-index in relation to cognitive dysfunction, we had a rationale to put ALPS-index in the mediation analysis. In the mediation analysis, we found that the ALPS-index is a significant mediator in the relationship between amyloid and tau protein deposition and cognitive dysfunction in multiple brain regions. Moreover, glymphatic failure or impairment preceding significant amyloid-β deposits was reported by a recent study.[42] Our results might indicate that ALPS-index mediates the cognitive dysfunction related to amyloid and tau deposition.

ALPS-index mediates AD-related cognitive impairment even after adjusting for the contribution of GM atrophy

Jack et al hypothesized a dynamic model of the Alzheimer pathological cascade, showing that sequential amyloid–tau neurodegeneration changes result in cognitive decline.[4] In addition, GM atrophy as well as amyloid and tau markers are independent factors for predicting cognitive decline in patients with mild cognitive impairment.[43] In the current study, we found that ALPS-index functioned as a significant mediator of cognitive dysfunction after correction for regional GMV ratios in the anterior/posterior cingulate cortex, precuneus, and frontal and sensory–motor cortices. This finding indicates that in the parietal, temporal, and occipital regions, the GMV had significant contributions to AD-related cognitive dysfunction. However, glymphatic activity played an important role in anterior/posterior cingulate cortex-, precuneus-, and frontal region-related cognitive dysfunction. These regions are responsible for attention, memory, and executive function, which are vulnerable to sleep deprivation.[44] Our findings are consistent with the relationship between slow-wave sleep, β-amyloid clearance, and cognitive dysfunction and the glymphatic system.[45] Recently, several studies have shown that significantly enhanced glymphatic activity can reduce amyloid burden and improve memory in an AD mouse model.[46,47] Thus, our findings may provide alternative biomarkers to evaluate treatment effects in patients with AD through indicators of modulation of glymphatic activity.

3.3.Limitations

First, the correlation of ALPS-index with human glymphatic function has not yet been substantially and rigorously validated by pathophysiological studies. Thus, we should cautiously interpret the relationship between the ALPS-index and glymphatic clearance. In addition, there are only a few direct comparisons of glymphatic activity measurements between different imaging modalities and diffusion MRI methods.[11] However, Zhang et al

have made a validation study for ALPS method, and they found a strong correlation between the ALPS-index and the intrathecal contrast media administration method to evaluate glymphatic function.[11] Second, our study is a cross-sectional study with a small sample size, and thus, our findings must be interpreted cautiously. Future studies should focus on the longitudinal changes in ALPS-indexes and their interactions with amyloid and tau protein deposition and cognitive dysfunction. Third, we did not measure the effects of sleep parameters, cardiovascular factors, or medications on the glymphatic system, which might have some interactions with glymphatic activity in our patients.[6] Last, the ALPS-index is a biomarker of glymphatic function representative of the whole brain rather than a regional function measurement. In the early stages of AD, the deposition of amyloid and tau proteins is relatively focal rather than global, which leads to the ALPS-index being less sensitive in detecting early AD. Thus, a significant change in ALPS-index occurred later than the deposition of amyloid and tau proteins in patients with AD. This might be a technique limitation that renders the glymphatic activity measured by ALPS-index less sensitive than the deposition of amyloid measured by PET image in our sequential analysis. Nevertheless, DTI-ALPS is a robust method to evaluate glymphatic activity even by different scanners.[48] Several methods have been proposed to measure glymphatic activity in the brain, which may have the potential to accurately estimate regional glymphatic function.[49,50] Improving the measurement of regional glymphatic function is our future goal.

3.4.Conclusions

ALPS-index is a significant mediator in the relationship between the deposition of amyloid and tau proteins and cognitive impairment, which may indicate that glymphatic dysfunction contributes to the pathogenesis of AD. Our findings further extend the clinical application of ALPS-index in the field of neurodegenerative studies and treatments.

Acknowledgments

This study was financially supported by grants from the Taiwanese Ministry of Health and Welfare (MOHW110-TDU-B-212-124005), Ministry of Science and Technology (MOST 108-2314-B-182A-023-, MOST 109-2314-B-182A-042-), and Chang Gung Memorial Hospital Research Fund (CMRPVVJ0352, CMRPVVJ0353, CMRPG3J0363, CMRPG3J0373). APRINOIA APN-1607 (PM-PBB3) has been registered as "florzolotau (^{18}F)" at the World Health Organization. The precursors used in the synthesis of ^{18}F-florzolotau were generously provided by APRINOIA Therapeutics. The authors acknowledge the administrative support of the Neuroscience Research Center, Chang Gung Memorial Hospital, Linkou, and Chang Gung Memorial Hospital Clinical Trial Center, which is funded by the Taiwanese Ministry of Health and Welfare (grants MOHW110-TDU-B-212-124005).

Author Contributions

J.-L.H. and Y.-C.W. contributed to the conception and design of the study; J.-L.H., C.H.T., K.-J.L., I.-T.H., and T.-C.Y. contributed to the acquisition and analysis of data; J.-L.H., M.-F.L., and L.-S.R. contributed to drafting the text or preparing the figures.

Potential Conflicts of Interest

T.-C.Y. owns equity of APRINOIA Therapeutics. The other authors declare no conflicts of interest.

Data Availability

All data and algorithms used in this study are included in the article or will be available upon request.

References

1. Oshio K. What is the "glymphatic system"? Magn Reson Med Sci 2021.
2. Iliff JJ, Wang M, Liao Y, et al. A paravascular pathway facilitates CSF flow through the brain parenchyma and the clearance of interstitial solutes, including amyloid beta. Sci Transl Med 2012;4:147ra11.
3. Harrison IF, Ismail O, Machhada A, et al. Impaired glymphatic function and clearance of tau in an Alzheimer's disease model. Brain 2020;143:2576–2593.
4. Jack CR Jr, Knopman DS, Jagust WJ, et al. Tracking pathophysiological processes in Alzheimer's disease: an updated hypothetical model of dynamic biomarkers. Lancet Neurol 2013;12:207–216.
5. Jack CR Jr, Bennett DA, Blennow K, et al. NIA-AA research framework: toward a biological definition of Alzheimer's disease. Alzheimers Dement 2018;14:535–562.
6. Nedergaard M, Goldman SA. Glymphatic failure as a final common pathway to dementia. Science 2020;370:50–56.
7. Taoka T, Naganawa S. Neurofluid dynamics and the glymphatic system: a neuroimaging perspective. Korean J Radiol 2020;21:1199–1209.
8. Ringstad G, Vatnehol SAS, Eide PK. Glymphatic MRI in idiopathic normal pressure hydrocephalus. Brain 2017;140:2691–2705.
9. Naganawa S, Nakane T, Kawai H, Taoka T. Age dependence of gadolinium leakage from the cortical veins into the cerebrospinal fluid assessed with whole brain 3D-real inversion recovery MR imaging. Magn Reson Med Sci 2019;18:163–169.
10. Taoka T, Masutani Y, Kawai H, et al. Evaluation of glymphatic system activity with the diffusion MR technique: diffusion tensor image analysis along the perivascular space (DTI-ALPS) in Alzheimer's disease cases. Jpn J Radiol 2017;35:172–178.
11. Zhang W, Zhou Y, Wang J, et al. Glymphatic clearance function in patients with cerebral small vessel disease. Neuroimage 2021;238:118257.
12. Siow TY, Toh CH, Hsu JL, et al. Association of sleep, neuropsychological performance, and gray matter volume with glymphatic

function in community-dwelling older adults. Neurology 2022;98: e829–e838.

13. Yang G, Deng N, Liu Y, et al. Evaluation of glymphatic system using diffusion MR technique in T2DM cases. Front Hum Neurosci 2020; 14:300.
14. Bae YJ, Choi BS, Kim JM, et al. Altered glymphatic system in idiopathic normal pressure hydrocephalus. Parkinsonism Relat Disord 2021, 82:56–60.
15. Chen HL, Chen PC, Lu CH, et al. Associations among cognitive functions, plasma DNA, and diffusion tensor image along the perivascular space (DTI-ALPS) in patients with Parkinson's disease. Oxid Med Cell Longev 2021;2021:4034509.
16. Carotenuto A, Cacciaguerra L, Pagani E, et al. Glymphatic system impairment in multiple sclerosis: relation with brain damage and disability. Brain 2022;145:2785–2795.
17. Toh CH, Siow TY. Glymphatic dysfunction in patients with ischemic stroke. Front Aging Neurosci 2021;13:756249.
18. Rossetti HC, Munro Cullum C, Hynan LS, Lacritz LH. The CERAD Neuropsychologic Battery Total Score and the progression of Alzheimer disease. Alzheimer Dis Assoc Disord 2010;24:138–142.
19. Morris JC, Heyman A, Mohs RC, et al. The consortium to establish a registry for Alzheimer's disease (CERAD). Part I. Clinical and neuropsychological assessment of Alzheimer's disease. Neurology 1989; 39:1159–1165.
20. Folstein MF, Folstein SE, McHugh PR. "Mini-mental state". A practical method for grading the cognitive state of patients for the clinician. J Psychiatr Res 1975;12:189–198.
21. Hughes CP, Berg L, Danziger WL, et al. A new clinical scale for the staging of dementia. Br J Psychiatry 1982;140:566–572.
22. Hsu JL, Hsu WC, Chang CC, et al. Everyday cognition scales are related to cognitive function in the early stage of probable Alzheimer's disease and FDG-PET findings. Sci Rep 2017;7:1719.
23. Liao YC, Lee WJ, Hwang JP, et al. ABCA7 gene and the risk of Alzheimer's disease in Han Chinese in Taiwan. Neurobiol Aging 2014;35:2423.e7–2423.e13.
24. Lin KJ, Hsu WC, Hsiao IT, et al. Whole-body biodistribution and brain PET imaging with [18F]AV-45, a novel amyloid imaging agent—a pilot study. Nucl Med Biol 2010;37:497–508.
25. Weng CC, Hsiao IT, Yang QF, et al. Characterization of ^{18}F-PM-PBB3 (^{18}F-APN-1607) uptake in the rTg4510 mouse model of tauopathy. Molecules 2020;25:1750.
26. Ashburner J, Friston KJ. Unified segmentation. Neuroimage 2005; 26:839–851.
27. Gonzalez-Escamilla G, Lange C, Teipel S, et al. Alzheimer's disease neuroimaging I. PETPVE12: an SPM toolbox for partial volume effects correction in brain PET—application to amyloid imaging with AV45-PET. Neuroimage 2017;147:669–677.
28. Ashburner J, Friston KJ. Diffeomorphic registration using geodesic shooting and Gauss-Newton optimisation. Neuroimage 2011;55:954–967.
29. Southekal S, Devous MD Sr, Kennedy I, et al. Flortaucipir F 18 quantitation using parametric estimation of reference signal intensity. J Nucl Med 2018;59:944–951.
30. Frazier JA, Chiu S, Breeze JL, et al. Structural brain magnetic resonance imaging of limbic and thalamic volumes in pediatric bipolar disorder. Am J Psychiatry 2005;162:1256–1265.
31. Leemans AJ, Jeurissen B, Sijbers J, Jones DK. ExploreDTI: a graphical toolbox for processing, analyzing, and visualizing diffusion MR data. *Proceedings of the 17th Annual Meeting of International Society for Magnetic Resonance in Medicine*. Hawaii, USA, 2009.
32. Basser PJ, Mattiello J, LeBihan D. MR diffusion tensor spectroscopy and imaging. Biophys J 1994;66:259–267.
33. MacKinnon DP, Valente MJ, Gonzalez O. The correspondence between causal and traditional mediation analysis: the link is the mediator by treatment interaction. Prev Sci 2020;21:147–157.
34. Hayes AF. *Introduction to mediation, moderation, and conditional process analysis: a regression-based approach*. 2nd ed. New York, NY: Guilford Press, 2018.
35. Steward CE, Venkatraman VK, Lui E, et al. Assessment of the DTI-ALPS parameter along the perivascular space in older adults at risk of dementia. J Neuroimaging 2021;31:569–578.
36. Siow TY, Toh CH, Hsu JL, et al. Association of sleep, neuropsychological performance, and gray matter volume with glymphatic function in community-dwelling older adults. Neurology 2022;98: e829–e838.
37. Tarasoff-Conway JM, Carare RO, Osorio RS, et al. Clearance systems in the brain—implications for Alzheimer disease. Nat Rev Neurol 2015;11:457–470.
38. Benveniste H, Lee H, Volkow ND. The glymphatic pathway: waste removal from the CNS via cerebrospinal fluid transport. Neuroscientist 2017;23:454–465.
39. Chandra A, Valkimadi PE, Pagano G, et al. Applications of amyloid, tau, and neuroinflammation PET imaging to Alzheimer's disease and mild cognitive impairment. Hum Brain Mapp 2019;40:5424–5442.
40. Doraiswamy PM, Sperling RA, Johnson K, et al. Florbetapir F 18 amyloid PET and 36-month cognitive decline: a prospective multicenter study. Mol Psychiatry 2014;19:1044–1051.
41. Hsu JL, Lin KJ, Hsiao IT, et al. The imaging features and clinical associations of a novel tau PET tracer-18F-APN1607 in Alzheimer disease. Clin Nucl Med 2020;45:747–756.
42. Peng W, Achariyar TM, Li B, et al. Suppression of glymphatic fluid transport in a mouse model of Alzheimer's disease. Neurobiol Dis 2016;93:215–225.
43. Malpetti M, Kievit RA, Passamonti L, et al. Microglial activation and tau burden predict cognitive decline in Alzheimer's disease. Brain 2020;143:1588–1602.
44. Durmer JS, Dinges DF. Neurocognitive consequences of sleep deprivation. Semin Neurol 2005;25:117–129.
45. Mander BA, Marks SM, Vogel JW, et al. Beta-amyloid disrupts human NREM slow waves and related hippocampus-dependent memory consolidation. Nat Neurosci 2015;18:1051–1057.
46. Lee Y, Choi Y, Park EJ, et al. Improvement of glymphatic-lymphatic drainage of beta-amyloid by focused ultrasound in Alzheimer's disease model. Sci Rep 2020;10:16144.
47. Zhang Y, Gruber R. Can slow-wave sleep enhancement improve memory? A review of current approaches and cognitive outcomes. Yale J Biol Med 2019;92:63–80.
48. Taoka T, Ito R, Nakamichi R, et al. Reproducibility of diffusion tensor image analysis along the perivascular space (DTI-ALPS) for evaluating interstitial fluid diffusivity and glymphatic function: CHanges in Alps index on multiple conditiON acquIsition eXperiment (CHAMONIX) study. Jpn J Radiol 2022;40:147–158.
49. Watts R, Steinklein JM, Waldman L, et al. Measuring glymphatic flow in man using quantitative contrast-enhanced MRI. AJNR Am J Neuroradiol 2019;40:648–651.
50. Naganawa S, Taoka T. The glymphatic system: a review of the challenges in visualizing its structure and function with MR imaging. Magn Reson Med Sci 2022;21:182–194.